

# Electron Mediation through the Thiocyanate Bridge: Mono- and Dinuclear Ruthenium Diimine Complexes and Their Mixed-Valence Properties<sup>1a</sup>

Vaithianathan Palaniappan,<sup>1b</sup> Sokki Sathaiah,<sup>1c</sup> Hari Dutt Bist,<sup>1c</sup> and Umesh Chandra Agarwala\*<sup>1b</sup>

Contribution from the Department of Chemistry and Department of Physics, Indian Institute of Technology, Kanpur 208 016, India. Received August 21, 1987

**Abstract:** Monomeric and thiocyanato bridged dimeric complexes of bis(bipyridine)ruthenium(II)/(III) complexes and their mixed valence analogues were synthesized and characterized by various physicochemical techniques. The cyclic voltammogram of the thiocyanate bridged (22) compound showed two overlapping waves corresponding to the successive oxidations (22) → (23) → (33), from which the comproportionation constant,  $K_{\text{com}}$ , was calculated. The interaction between metal centers via thiocyanate ion occurs through a  $d\pi(\text{Ru})-3\pi^*(\text{NCS})-d\pi(\text{Ru})$  overlap. This interaction could be conveniently modified as to our needs by simply varying the coligands (in terms of  $\sigma/\pi$ -donor and  $\sigma/\pi$ -acceptor properties). Vibrational (IR and RR), electronic spectral and electrochemical properties and a possible relevance to multielectron redox catalysis are discussed.

The interest in the transition-metal diimine complexes comes from their utility as the multielectron redox catalysts ("electron sponges") in water oxidation reactions.<sup>2-4</sup> In the recent past<sup>5-7</sup> an enormous amount of investigations has been carried out, especially, on the ruthenium diimine complexes. Starting with an apparently simple compound,  $[\text{Ru}(\text{bpy})_3]^{2+}$ , which has received potential utility as a sensitizer for the photodissociation of water, the polymeric ruthenium diimine compounds are capable of oxidizing water by a multielectron process without the addition of an external catalyst like  $\text{RuO}_2$  and have been found to be active as redox catalysts for the oxidations of water to dioxygen,<sup>5,6</sup> or chloride to chlorine,<sup>8</sup> and of several organic substrates.<sup>9</sup>

The results of extensive investigations by Ludi,<sup>10,11</sup> Meyer,<sup>12,13</sup> and Taube<sup>14-16</sup> and their co-workers have provided a basis for

understanding the interesting properties and mixed-valence behavior of discrete polynuclear transition-metal complexes. Mainly with  $[\text{Ru}(\text{NH}_3)_5]^{n+}$ ,  $[\text{Fe}(\text{CN})_5]^{n-}$ , and  $[\text{Ru}(\text{bpy})_2]^{n+}$  as building blocks and with a variety of bridging units, a large number of compounds were synthesized and studied in terms of the inter-valence transfer (IT) transition, a metal-to-metal charge transfer (MMCT). The extent of communication between the metal centers in these complexes, a crucial factor in determining their utility as catalysts in multielectron transfer processes, was evaluated by using the IT spectral data and the conceptual model proposed by Hush.<sup>17</sup> Depending on the nature of the metal centers, the bridging ligands, and the distance between them, a wide range of metal-to-metal interactions (from a delocalized class III to weakly coupled class II behavior) were encountered<sup>16</sup> in these complexes.

The feasibility of chalcogenocyanate ions acting as the bridging species in such compounds was established recently.<sup>18-20</sup> Thiocyanate and selenocyanate ions were observed to mediate a valence delocalization between  $[\text{Ru}(\text{NH}_3)_5]^{n+}$ <sup>18</sup> and  $[\text{Fe}(\text{CN})_5]^{n-}$  units.<sup>19</sup> They underwent successive oxidation to (23) and (33) from (22) within a relatively shorter range of potential suggesting their catalytic potentiality in multielectron transfer processes. It was also proposed therein (1) that the anionic nature of the bridging unit could increase the electrostatic contribution,  $\Delta G^{\circ}_{\text{coul}}$ , to the total stability of the mixed-valence states,  $\Delta G^{\circ}_{\text{tot}}$ , in these compounds<sup>19</sup> and (2) that the observed decrease in the values of the delocalization parameter,  $\alpha^2$  of  $[(\text{CN})_5\text{Fe}-\text{NCS}-\text{Fe}(\text{CN})_5]^{6-}$ , where X = S or Se, compared to that of  $[(\text{NH}_3)_5\text{Ru}-\text{NCS}-\text{Ru}(\text{NH}_3)_5]^{4+}$  and hence the extent of delocalization of the optical electron could be attributed to two cooperative factors: (i) a poorer overlap of the  $d\pi(\text{M})-3\pi^*(\text{NCS})-d\pi(\text{M})$  unit, when going from ruthenium to iron and (ii) a good  $\pi$ -acceptor ligand, like  $\text{CN}^-$  ion in the case of  $[\text{Fe}(\text{CN})_5]^{n-}$ , could impart enough restriction to the delocalization of the optical electron over the  $[\text{FeNCSFe}]$  unit.

It was thus speculated that the extent of communication between the metal centers in the case of  $[\text{Cl}(\text{bpy})_2\text{RuNCSRu}(\text{bpy})_2\text{Cl}]^{2+}$  should be considerably smaller compared to that of  $[(\text{NH}_3)_5\text{RuNCSRu}(\text{NH}_3)_5]^{4+}$  due to the  $\pi$ -acidity of the 2,2'-bipyridine coligands. Further, the metal-to-metal interaction could

(1) (a) (22), (23), and (33) represent the three different oxidation states for the dimeric compounds, and bpy represents 2,2'-bipyridine. (b) Department of Chemistry. (c) Department of Physics.

(2) Kalyanasundaram, K. *Coord. Chem. Rev.* **1982**, *46*, 159.

(3) (a) Ramaraj, R.; Kira, A.; Kaneko, M. *J. Chem. Soc., Faraday Trans. 1986*, *182*. (b) Ramaraj, R.; Kira, A.; Kaneko, M. *Angew. Chem., Int. Ed. Engl.* **1986**, *25*, 825, 1009.

(4) (a) Grätzel, M. In *Energy Resources through Photochemistry and Catalysis*; Academic Press: New York, 1983. (b) Grätzel, M. *Acc. Chem. Res.* **1981**, *14*, 376.

(5) Seddon, E. A.; Seddon, K. R. In *Topics In Inorganic and General Chemistry—Monograph 19: The Chemistry of Ruthenium*; Clark, R. J. H., Ed.; Elsevier: Amsterdam, 1984; pp 1173-1256.

(6) Gilbert, J. A.; Eggleston, D. S.; Murphy, W. R., Jr.; Geselowitz, D. A.; Gersten, S. W.; Hodgson, D. R.; Meyer, T. J. *J. Am. Chem. Soc.* **1985**, *107*, 3855.

(7) (a) Gilbert, J. A.; Geselowitz, D. A.; Meyer, T. J. *J. Am. Chem. Soc.* **1986**, *108*, 1493. (b) Murphy, W. R., Jr.; Takeuchi, K.; Barley, M. H.; Meyer, T. J. *Inorg. Chem.* **1986**, *25*, 1041.

(8) (a) Ellis, C. D.; Gilbert, J. A.; Murphy, W. R., Jr.; Meyer, T. J. *J. Am. Chem. Soc.* **1983**, *105*, 4842. (b) Vining, W. J.; Meyer, T. J. *Inorg. Chem.* **1986**, *25*, 2023.

(9) Roecker, L.; Meyer, T. J. *J. Am. Chem. Soc.* **1986**, *108*, 4066.

(10) Glauser, R.; Hauser, U.; Herren, F.; Ludi, A.; Roder, P.; Schmidt, E.; Siegnhaler, H.; Wenk, F. *J. Am. Chem. Soc.* **1973**, *95*, 8457.

(11) (a) Felix, F.; Ludi, A. *Inorg. Chem.* **1978**, *17*, 1782. (b) Furholz, U.; Bürgi, H. B.; Wagner, F. E.; Stebler, A.; Ammeter, J. H.; Krausz, E.; Clark, R. J. H.; Stead, M. J.; Ludi, A. *J. Am. Chem. Soc.* **1984**, *106*, 121. (c) Joss, S.; Bürgi, H. B.; Ludi, A. *Inorg. Chem.* **1985**, *24*, 949.

(12) (a) Meyer, T. J. *Chem. Phys. Lett.* **1979**, *64*, 417. (b) Powers, M. J.; Meyer, T. J. *J. Am. Chem. Soc.* **1980**, *102*, 1289. (c) Curtis, J. C.; Meyer, T. J. *Inorg. Chem.* **1982**, *21*, 1562. (d) Goldsby, K. A.; Meyer, T. J. *Inorg. Chem.* **1984**, *23*, 3002.

(13) Meyer, T. J. *Ann. N. Y. Acad. Sci.* **1978**, *313*, 496. (b) Meyer, T. J. In *Mixed Valence Compounds*; Brown, D., Ed.; D. Reidel: Dordrecht, The Netherlands, 1980; p 75. (c) Meyer, T. J. In *Mechanistic Aspects of Inorganic Reactions*; Rorabacher, D. B., Endicott, J. F., Eds.; American Chemical Society: Washington, DC, 1982; ACS Symp. Ser. No. 198, p 137.

(14) Richardson, D. E.; Taube, H. *Coord. Chem. Rev.* **1984**, *60*, 107.

(15) Taube, H. *Angew. Chem., Int. Ed. Engl.* **1984**, *23*, 329.

(16) Creutz, C. *Prog. Inorg. Chem.* **1983**, *30*, 1.

(17) (a) Hush, N. S. *Trans. Faraday Soc.* **1961**, *57*, 557. (b) Hush, N. S. *Prog. Inorg. Chem.* **1967**, *8*, 391. (c) Hush, N. S. *Electrochim. Acta* **1968**, *13*, 1005.

(18) Palaniappan, V.; Yadav, S. K. S.; Agarwala, U. C. *Polyhedron* **1985**, *4*, 1457.

(19) Palaniappan, V.; Singru, R. M.; Agarwala, U. C. *Inorg. Chem.* **1988**, *27*, 181.

be "tuned" as to our needs by simply varying (in terms of  $\sigma/\pi$ -acceptor/-donor properties) the coligands on the metal centers. This tunability of the electron mediation by the bridging ligands will have a large impact on the development of multielectron redox catalysts.

Thus, in continuation of our earlier efforts, a study on the thiocyanate-bridged mixed-valence compounds having  $[(bpy)_2Ru]^{n+}$  as the building block was undertaken, the results of which are presented in this paper.

### Experimental Section

**Materials.** The complexes *cis*- $[(bpy)_2RuCl_2] \cdot 2H_2O$ ,<sup>21</sup>  $[(bpy)_2Ru(NO)Cl](PF_6)_2$ ,  $[(bpy)_2Ru(NO)(NO_2)](PF_6)_2$ ,<sup>22</sup> and  $[(bpy)_2Ru(NCS)_2]$ <sup>23</sup> were prepared and purified as described in the literature. Laboratory reagent grade ammonium hexafluorophosphate (Janssen Chimica), sodium tetraphenylborate and potassium thiocyanate (Sisco), sodium perchlorate (Riedel), potassium selenocyanate (Fluka AG), and AR grade potassium azide were procured and used as such. Solvents were dried by standard procedures<sup>24a</sup> and distilled before use. Doubly distilled water was used wherever mentioned. Ce(IV) perchlorate solution was prepared from Ce(IV) hydroxide and 6 M perchloric acid<sup>24b</sup> and analyzed spectrophotometrically.

**Preparations.** (a)  $[(bpy)_2Ru(NCS)Cl]$ . This compound was prepared by two different procedures.

(A) The complex  $[(bpy)_2Ru(NO)Cl](PF_6)_2$  (202.3 mg, 0.263 mmol) was dissolved in acetone (20–25 mL) and protected from light. An equimolar amount of  $KN_3$  (21.4 mg) dissolved in methanol was added dropwise with stirring, producing the purple solvenato complex,  $[(bpy)_2Ru(aceton)Cl]^+$ . A saturated methanolic solution of potassium thiocyanate was added to this, and the resulting solution was stirred for an hour. The resulting solution was filtered into excess of diethyl ether with stirring, and the precipitated crude product was filtered and washed extensively with water to remove the unreacted potassium thiocyanate and then with ether. Recrystallization from methylene chloride/diethyl ether yielded a dark purple product (yield = 70–80%). It was further purified by gel filtration through Sephadex LH-20 resin as follows. A concentrated solution of the recrystallized product in 5–10 mL of acetonitrile was sorbed onto the column (50 × 2 cm) top. Slowest possible elution with acetonitrile:methylene chloride (1:1) resolved two bands on the column. On the basis of retention times, the compound from the major second band was identified to be the desired monomeric product. This was separated out by precipitation with excess of diethyl ether from the eluate: yield 60%.

(B) A suspension of *cis*- $[(bpy)_2RuCl_2] \cdot 2H_2O$  (100 mg) in 15–20 mL of water was refluxed with vigorous stirring for 20–25 min. The resulting red brown  $[(bpy)_2Ru(H_2O)Cl]^+$  solution was filtered through a fine porosity glass frit and cooled to room temperature. An aqueous solution (5–10 mL) of excess potassium thiocyanate (~0.5 g) was added with stirring, and the dark colored crude product which immediately precipitated was filtered and washed well with water. This was purified as described earlier in a(A) by gel filtration through Sephadex LH-20 column. The band that moved in a major amount was eluted with acetonitrile:methylene chloride or acetonitrile:benzene mixture (1:1). The compound was precipitated from the concentrated eluate by adding excess of diethyl ether: yield 75–85%. Another small band moved through the column was identified to be  $[(bpy)_2Ru(SCN)Cl]$  based on the position and integrated intensity of  $\nu(CN)$  band in the vibrational spectrum.<sup>25</sup> Anal. Calcd for  $C_{21}ClH_{20}N_5O_2RuS$ : C, 46.41; H, 3.68; N, 12.89; Cl, 6.63; S, 5.89. Found: C, 46.73; H, 3.74; N, 12.53; Cl, 6.60; S, 5.23.

(b)  $[Cl(bpy)_2RuNCSRu(bpy)_2]X$  ( $X^- = BPh_4^-$ ,  $ClO_4^-$ , or  $PF_6^-$ ). An aqueous solution of  $[(bpy)_2Ru(H_2O)Cl]^+$  was prepared from *cis*- $[(bpy)_2RuCl_2] \cdot 2H_2O$  as described in a(B). To this was added a stoichiometrically equimolar amount of  $[(bpy)_2Ru(NCS)Cl] \cdot 2H_2O$  (100 mg)

in 15–20 mL of ethanol. The resulting mixture was degassed by bubbling dinitrogen (10–15 min), and the solution was refluxed for 2.5 h with a continual stream of dinitrogen over the mixture. The solution was filtered into an aqueous solution of sodium tetraphenylborate, sodium perchlorate, or ammonium hexafluorophosphate. The flocculant red brown precipitate was filtered, washed with water, and dried; yield = 90–95%. Chromatographic purification of the complex was carried out by using alumina column (50 × 3 cm). A concentrated solution of the crude product in acetonitrile was charged onto the column. The elution was carried out by using acetonitrile:methylene chloride or acetonitrile:benzene mixture (1:9, v/v) and slowly enriching acetonitrile in the mixture to (4:6) proportion. The major portion of the compound moved as a single band, which was eluted and precipitated: yield = 80–85%. Minor amount of monomeric impurities were discarded.

The same compound was also prepared by refluxing 2:1 stoichiometric mixture of *cis*- $[(bpy)_2RuCl_2] \cdot 2H_2O$  and potassium thiocyanate in ethanol for 60–72 h. The crude product was purified by alumina column chromatography as described in the earlier paragraph. Anal. Calcd for  $BC_{65}Cl_2H_{52}N_9Ru_2S$ : C, 61.17; H, 4.09; N, 9.88. Found: C, 61.83; H, 4.00; N, 10.21.

(c)  $[Cl(bpy)_2RuNCSRu(bpy)_2(NCS)]BPh_4$ . Fifteen milliliters of an aqueous solution of  $[(bpy)_2Ru(H_2O)Cl]^+$  was prepared from *cis*- $[(bpy)_2RuCl_2] \cdot 2H_2O$  (52 mg) as described in a(B). An equimolar amount of *cis*- $[(bpy)_2Ru(NCS)_2]$  in ethanol (10 mL) was added, and the resulting solution was refluxed for 2 h. The solution was filtered into an aqueous solution of sodium tetraphenylborate. The red brown precipitate formed in quantitative yield was filtered, washed successively with water and ether, and dried in vacuum. Anal. Calcd for  $BC_{66}ClH_{52}N_{10}Ru_2S_2$ : C, 61.06; H, 4.01; N, 10.79. Found: C, 60.54; H, 4.20; N, 11.05.

(d)  $[Cl(bpy)_2RuNCSRu(bpy)_2(NO_2)]BPh_4$ . The dark brown colored solvenato complex  $[(bpy)_2Ru(aceton)(NO_2)]^+$  was prepared from  $[(bpy)_2Ru(NO)(NO_2)](PF_6)_2$  (194 mg) as described earlier (cf. a(A)). A stoichiometrically equimolar amount of  $[(bpy)_2Ru(NCS)Cl] \cdot 2H_2O$  (136 mg) in ethanol acetone mixture (1:1) (20–25 mL) was added to this, and the solution was refluxed for 2–2.5 h. The resulting solution was processed as described in (c). The compounds obtained by procedures (c) and (d) were purified by recrystallization from acetone/diethyl ether and finally by alumina column chromatography. The major dimeric products were eluted and precipitated by using excess of ether, and the minor amounts of unreacted monomeric compounds were discarded. Anal. Calcd for  $BC_{65}ClH_{52}N_{10}O_2Ru_2S$ : C, 60.70; H, 4.05; N, 10.90. Found: C, 60.22; H, 3.84; N, 11.09.

(e)  $[(bpy)_2Ru(NCS)Cl]X$  ( $X^- = PF_6^-$  or  $BPh_4^-$ ). The oxidation of the Ru(II) compound was carried out by using Ce(IV) perchlorate solution. A stoichiometrically equimolar solution of Ce(IV) was added with stirring to a solution of  $[(bpy)_2Ru(NCS)Cl]$  in acetone, kept in dark. The stirring was continued for an hour. Excess of the anion (sodium tetraphenylborate or ammonium hexafluorophosphate) was added to this, and the solution was filtered into excess of diethyl ether with stirring. The flocculant purple brown to dark brown colored precipitate was filtered and washed extensively with water and then with ether. The compound was recrystallized with acetone/diethyl ether: yield = 85–90%. The compound purity was further checked by passing it through Sephadex LH-20 column, where it showed a single band. Anal. Calcd for  $BC_{45}ClH_{36}N_5RuS$ : C, 65.37; H, 4.36; N, 8.47. Found: C, 65.07; H, 4.05; N, 8.87.

(f)  $[Cl(bpy)_2RuNCSRu(bpy)_2X](BPh_4)_3$  ( $X^- = Cl^-$ ,  $NCS^-$ , or  $NO_2^-$ ). An acetone (10–15 mL) solution of  $[Cl(bpy)_2RuSCNRu(bpy)_2X]BPh_4$  (100 mg) was protected from light. A solution containing a little more than stoichiometrically 2 equiv of Ce(IV) was added with stirring, and the stirring was continued for an hour. To the resulting solution excess of solid sodium tetraphenylborate was added. The solution was then filtered into an excess of diethyl ether with stirring whereupon a flocculant red orange precipitate was formed in almost quantitative yield. This was filtered and washed well with water (4 × 10 mL portions) and finally with ether. Anal. Calcd for  $[Cl(bpy)_2RuNCSRu(bpy)_2(NCS)](BPh_4)_3$ : C, 70.70; H, 4.75; N, 7.24. Found: C, 69.95; H, 4.30; N, 8.00. Calcd for  $[Cl(bpy)_2RuNCSRu(bpy)_2NO_2](BPh_4)_3$ : C, 70.51; H, 4.78; N, 7.28. Found: C, 70.95; H, 4.25; N, 7.33.

(g)  $[Cl(bpy)_2RuNCSRu(bpy)_2Cl](BPh_4)_2$ . The mixed-valence species was prepared by either oxidizing the (22) compound with 1 equiv of Ce(IV) solution or by mixing equimolar amounts of (22) and (33) compounds in acetonitrile. The tetraphenylborate salt, separated out from these solutions, was not stable for longer periods, and consistent micro-analytical results could not be obtained.

(h)  $[Cl(bpy)_2RuNCSRu(bpy)_2X]^{2+}$  ( $X^- = NO_2^-$  or  $NCS^-$ ). The mixed valence species in these cases were generated in situ by Ce(IV) or  $[Fe(bpy)_3]^{3+}$  oxidation.<sup>26</sup>

(20) Palaniappan, V.; Agarwala, U. C. *Inorg. Chem.*, accepted for publication.

(21) Sullivan, B. P.; Salmon, D. J.; Meyer, T. J. *Inorg. Chem.* **1978**, *17*, 3334.

(22) Goodwin, J. B.; Meyer, T. J. *Inorg. Chem.* **1971**, *10*, 471.

(23) (a) Bryant, G. M.; Fergusson, J. E.; Powell, H. K. *J. Aust. J. Chem.* **1971**, *24*, 257. (b) Bryant, G. M.; Fergusson, J. E. *Aust. J. Chem.* **1971**, *24*, 275. (c) Johnson, E. C.; Callahan, R. W.; Eckberg, R. P.; Hatfield, W. E.; Meyer, T. J. *Inorg. Chem.* **1979**, *18*, 618.

(24) (a) Vogel, A. I. *Practical Organic Chemistry*, 2nd ed.; Longmans, Green and Co.: London, 1951. (b) Vogel, A. I. *A Textbook of Quantitative Inorganic Chemistry*, 2nd ed.; Longmans, Green and Co.: London, 1951.

(25) The integrated intensity, "A", of the CN stretching mode of the thiocyanate group was estimated by using Ramsay's method.<sup>33</sup> For dimeric compounds the values, viz.,  $25\text{--}40 \times 10^4 \text{ M}^{-1} \text{ cm}^2$ , were greater compared to that of the S-bonded/N-bonded compounds.

(26) Chang, J. P.; Fung, E. Y.; Curtis, J. C. *Inorg. Chem.* **1986**, *25*, 4233.

The perchlorate salts described were invariably associated with two or more molecules of water of crystallization.<sup>27</sup> The presence of the water molecules was verified by recording their <sup>1</sup>H NMR spectra in DMSO-*d*<sub>6</sub> solvent. The signal due to the lattice water molecules was observed at around 4.6–4.8 ppm. The tetraphenylborate salts of the compounds were preferred for the oxidation purposes as they provided less solubility problems when used in acetone solution. Because of the light-sensitive nature of the acetonitrile solution of 2,2'-bipyridine complexes of ruthenium, the preparation, workup, and purification steps were carried out generally in reduced light.

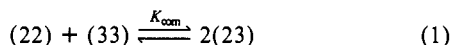
Caution should be observed in manipulating the perchlorate salts, wherever mentioned.

**Physicochemical Methods.** General description of the physicochemical and chromatographic methods is given elsewhere.<sup>28,29</sup> Near infrared spectra were recorded on a Hitachi MU-3400 spectrophotometer, by using matched 1-cm quartz cells. The extinction coefficients were calculated by recording the absorbance for at least two different concentrations of the solutions. The fluorescence and resonance Raman spectra were obtained by using the spectrophotometer described earlier.<sup>29b</sup> The spectra were obtained at right angles with samples in 1 mm i.d. capillary tubes. The relative intensities of the vibrational bands were obtained by comparing with the  $\nu(\text{CN})$  band of acetonitrile solvent at 2249  $\text{cm}^{-1}$ . The emission quantum yields could not be determined accurately as the samples underwent local burning due to high power of the exciting laser. However, assuming a similar burning rate and recording the emission spectra after approximately equal time intervals, the relative quantum efficiencies of the monomeric and dimeric compounds were obtained. The details of the CV measurements are given elsewhere.<sup>20</sup> The potentials are referenced to SCE.

## Results

**Monomeric and Dimeric Compounds.** The reactions of the chalcogenocyanate ions with the solvenato complexes  $[(\text{bpy})_2\text{Ru}(\text{sol})\text{Cl}]^+$  yielded the N-bonded chalcogenocyanate complexes in good yields. The possibility of the formation of the corresponding linkage isomers (S- or Se-bonded compounds) with  $\pi$ -acid coligands such as  $\text{CN}^-$ , bpy, and  $\text{PPh}_3$  has been ruled out by earlier workers.<sup>30,31</sup> However, the formation of a small amount of the S- or Se-bonded isomer was noticed in the reaction between the chalcogenocyanate ion with the solvenato complex  $[(\text{bpy})\text{Ru}(\text{sol})\text{Cl}]^+$ . Hence it is concluded that, although the  $\pi$ -acceptor nature of 2,2'-bipyridine coligand will favorably influence the formation of the N-bonded isomers, the formation of the S- or Se-bonded isomers cannot be strictly ruled out. This is borne out by the fact that the reaction of  $[(\text{NH}_3)_5\text{Ru}(\text{H}_2\text{O})]^{2+}/[(\text{NH}_3)_5\text{RuCl}]^{2+}$  (where the coligands are  $\sigma$ -donors) with the chalcogenocyanate ion yields both N- and S- or Se-bonded isomers. Further studies on the separated S- or Se-bonded isomers,  $[(\text{bpy})_2\text{Ru}(\text{XCN})\text{Cl}]$  (X = S or Se,<sup>20</sup> cf. Experimental a(B)), are under progress. The oxidation of compounds (22) was carried out in acetone solution with tetraphenylborate salts. The interconversions of hexafluorophosphate salts into chloride form before and after the oxidations were necessary<sup>32</sup> in the case of the hexafluorophosphate salts of the compounds. This was due to the solubility problems caused by the hexafluorophosphate anion in acetonitrile solution.

The mixed-valence compound prepared by the mixing of the (22) and (33) compounds (cf. Experimental Section (g)) contained considerable amounts of the unreacted (22) and (33) compounds. This is understandable as the comproportionation constant,  $K_{\text{com}}$ , for the reaction (1) is low. Hence, the in situ generation of (23)



species by the oxidation of (22) moiety with Ce(IV) was preferred.

Table I. Infrared Spectral Data in  $\text{cm}^{-1}$  a,c,d

$[(\text{bpy})_2\text{Ru}(\text{NCS})\text{Cl}] \cdot 2\text{H}_2\text{O}^b$	$[\text{Cl}(\text{bpy})_2\text{RuNCSRu}(\text{bpy})_2\text{Cl}]\text{BPh}_4$
2120 (vs) <sup>e</sup>	2150 (vs) <sup>f</sup>
810 (w)	777 <sup>g</sup>
660 (w)	665 (w)
485 (vw)	500 (w)
430 (br)	470 (vw)
380 (m)	435 (br)
360 (w)	365 (w)
330 (br)	330 (br)
285 (m)	290 (m)
265 (m)	260 (m)

<sup>a</sup> Unless otherwise stated the spectra were recorded in KBr and CsI disk. <sup>b</sup> Water of crystallization appeared as two characteristic peaks at around 3450 and 1640  $\text{cm}^{-1}$ . <sup>c</sup> Peaks characteristic of the coordinated 2,2'-bipyridine and the anion  $\text{BPh}_4^-$  were observed at their characteristic positions and are not given here. <sup>d</sup> The various peaks at low energies are assigned to the  $\nu(\text{M-S})$ ,  $\nu(\text{M-N})$ , and  $\nu(\text{M-Cl})$  modes of thiocyanate and 2,2'-bipyridine and chloro ligands. <sup>e</sup> The integrated intensity  $A_{(\text{CN})}$  of the  $\nu(\text{CN})$  band was calculated by using the Ramsay's method;<sup>33</sup>  $A_{(\text{CN})} = 12 \times 10^4 \text{ M}^{-1} \text{ cm}^{-2}$ .  $A_{(\text{CN})}$  value for  $[(\text{bpy})_2\text{Ru}(\text{NCS})_2]$  is  $10.1 \times 10^4 \text{ M}^{-1} \text{ cm}^{-2}$ <sup>30</sup> which is comparable with our value. <sup>f</sup>  $A_{(\text{CN})} = 25 \times 10^4 \text{ M}^{-1} \text{ cm}^{-2}$ . <sup>g</sup> The 740–800- $\text{cm}^{-1}$  region is masked by intense bands due to phenyl ring vibrational modes. The value was obtained from the Raman spectrum.

In the case of  $[\text{Cl}(\text{bpy})_2\text{RuNCSRu}(\text{bpy})_2\text{Cl}]^{2+}$ , (23) species was separated out as the tetraphenylborate salt. The extinction coefficient values calculated for the different bands in the electronic spectrum are based on the molecular weight corresponding to  $[\text{Cl}(\text{bpy})_2\text{RuNCSRu}(\text{bpy})_2\text{Cl}](\text{BPh}_4)_2$ .

**Infrared Spectra.** Infrared spectra of the compounds showed the characteristic bands for the coordinated 2,2'-bipyridine and thiocyanate ion. The mode of bonding of the thiocyanate ion in the monomeric complexes was established by the position<sup>28,29a</sup> and the integrated intensity (A) of the  $\nu(\text{CN})$  band<sup>33</sup> (cf. Table I). For the dimeric complexes, a shift of 20–25  $\text{cm}^{-1}$  toward the higher energy was observed in the position of the  $\nu(\text{CN})$  band, and the integrated intensity of the CN stretching band increased 3–5 times, compared to that of the monomeric compounds.<sup>25</sup> The compound,  $[\text{Cl}(\text{bpy})_2\text{RuSCNRu}(\text{bpy})_2(\text{NCS})]\text{BPh}_4$ , exhibited two bands at around 2160 and 2110  $\text{cm}^{-1}$  in the CN stretching region confirming the presence of the bridging and N-bonded thiocyanate ions. All the compounds exhibited the characteristic bands for the different anions and coligands like  $\text{NO}_2^-$  ion.

**Absorption and Emission Spectra.** The essential features of the absorption and emission spectral data are presented in Table II. The compounds exhibited the intraligand  $\pi$ - $\pi^*$  transition of the 2,2'-bipyridine at around 290 and 240 nm.<sup>23</sup> The extinction coefficient of the band at around 290 nm was found to be 25 000–35 000  $\text{M}^{-1} \text{ cm}^{-1}$  for monomeric bis(bipyridine) complexes and increased approximately by 2- and 3-fold for dimeric and trimeric compounds, respectively.<sup>23</sup> The metal-to-2,2'-bipyridine charge-transfer (MLCT) transition  $d\pi(\text{Ru})-\pi^*(\text{bpy})$  and  $d\pi(\text{Ru})-\pi_2^*(\text{bpy})$  were observed at around 500 and 340 nm. The interesting observation, however, is that the lower energy MLCT band exhibited invariably a shoulder of almost equal intensity at higher energies, in the case of monomers, and at lower energies, in the case of dimers. This shoulder, we attribute to the metal to thiocyanate  $d\pi(\text{Ru})-3\pi^*(\text{NCS}^-)$  charge transfer. This is substantiated by the fact that the lowest energy MLCT of the dithiocyanate compound,  $[\text{Cl}(\text{bpy})_2\text{RuNCSRu}(\text{bpy})_2\text{NCS}]\text{BPh}_4$ , exhibits a more prominent shoulder toward the lower energy region (Figure 3). The assignments are further corroborated by the resonance Raman studies of the complexes (vide supra). The prominent band of the lowest energy MLCT profile undergoes a blue shift<sup>23</sup> of around 600  $\text{cm}^{-1}$  in polar solvents (e.g.,  $\text{CH}_2\text{Cl}_2$  to acetonitrile) and a slight blue shift when going from a monomer to dimer. The shoulder corresponding to the metal-to-thiocyanate charge transfer was clearly visible in nonpolar solvents like methylene chloride (Figure 1). The second charge-transfer band

(27) In general, the perchlorate salts of these compounds absorb moisture as was observed by earlier workers.

(28) Palaniappan, V.; Agarwala, U. C. *Inorg. Chem.* **1986**, *25*, 4064.

(29) (a) Yadav, S. K. S.; Agarwala, U. C. *Polyhedron* **1984**, *3*, 1. (b) Lamba, O. P.; Bist, H. D.; Jain, Y. S. *Can. J. Chem.* **1983**, *61*, 608.

(30) Wajda, S.; Rachlewicz, K. *Inorg. Chim. Acta* **1978**, *31*, 35.

(31) (a) Gutterman, D. F.; Gray, H. B. *Inorg. Chem.* **1972**, *11*, 1727. (b) Huheey, J. E. *Inorganic Chemistry—Principles of Structure and Reactivity*, 2nd ed.; Harper International SI Edn.: Cambridge, 1983; pp 516–521.

(32) Callahan, R. W.; Keene, F. R.; Meyer, T. J.; Salmon, D. J. *J. Am. Chem. Soc.* **1977**, *99*, 1064.

(33) Norbury, A. H. *Adv. Inorg. Chem. Radiochem.* **1975**, *17*, 231.

**Table II.** Electronic Spectral Data for the Monomeric and Dimeric Bis(bipyridine)ruthenium(II)/(III) Complexes<sup>a</sup>

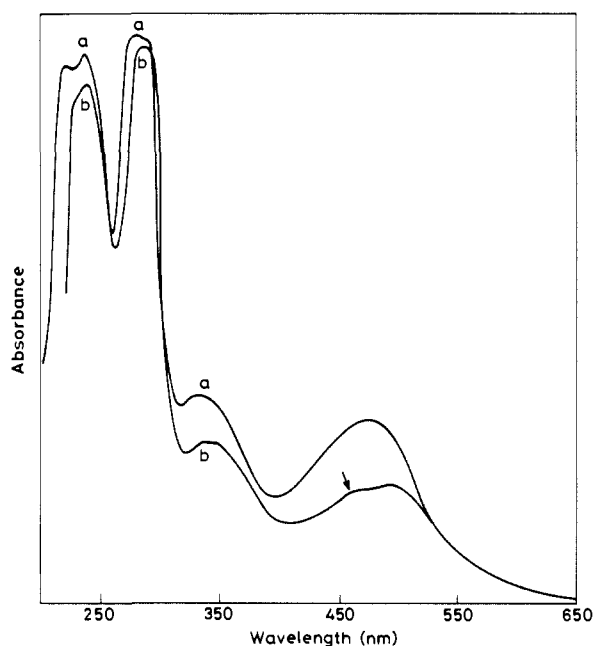
[(bpy) <sub>2</sub> Ru(NCS)Cl]		[(bpy) <sub>2</sub> Ru(NCS) <sub>2</sub> ]		[Cl(bpy) <sub>2</sub> RuNCSRu(bpy) <sub>2</sub> Cl] <sup>n+</sup> c,d		
Ru(II)	Ru(III)	Ru(II)	Ru(III) <sup>b</sup>	(22)	(23)	(33)
502 (4400)		597 (sh)	505 (sh)	525 (sh)	940 (411)	
460 (sh)	470 (6300)	515 (5700)	454 (4440)	455 (11365)	470 (13775)	428 (20510)
		440 (sh)	420 (sh)		460 (sh) (13700)	
330 (10200)	322 (sh) (10225)	375 (5700)	340 (sh) (6940)	330 (991)		325 (sh)
294 (42400)	292 (45450)	295 (37500)	289 (35160)	285 (58330)		285 (106300)
290 (39600)						
239 (32800)	242 (25300)	245 (32250)	243 (23640)	250 (sh)		242 (64200)
				240 (31580)		
215 (s)	217 (29250)	220 (s)	220 (25260)	212 (43000)		215 (80650)
$\lambda_{em}^g$				$\lambda_{em}^h$		
715, <sup>e</sup> 703 <sup>f</sup>				692, <sup>e</sup> 680 <sup>f</sup>		

<sup>a</sup> Wavelengths are in nm, and the extinction coefficients in M<sup>-1</sup> cm<sup>-1</sup> are given in parentheses; spectral data in acetonitrile solutions. <sup>b</sup> The perchlorate salt of the oxidized species. <sup>c</sup> Tetraphenylborate salt. <sup>d</sup> Data in UV region for the (23) compound was not obtained. <sup>e</sup>  $\lambda_{ex}$  = 514.5 nm. <sup>f</sup>  $\lambda_{ex}$  = 457.9 nm. <sup>g</sup>  $\Delta\bar{\nu}_{1/2}$  (fwhm) = 2350 cm<sup>-1</sup>. <sup>h</sup>  $\Delta\bar{\nu}_{1/2}$  (fwhm) = 2750 cm<sup>-1</sup>.

**Table III.** Solvent Dependent NIR Spectral Data for [Cl(bpy)<sub>2</sub>RuNCSRu(bpy)<sub>2</sub>Cl]<sup>2+</sup><sup>a</sup>

solvent	$(\frac{1}{n^2} - \frac{1}{D})^b$	$\bar{\nu}_{IT}$ (cm <sup>-1</sup> )	$\epsilon_{IT}$ (M <sup>-1</sup> cm <sup>-1</sup> )
water	0.546	10 000	
methanol	0.535	10 753	
acetonitrile	0.528	10 638	411
ethanol	0.499	10 256	
acetone	0.493	10 417	387
<i>N</i> -methyl formamide	0.483	10 309	
propylene carbonate	0.481	10 204	
<i>N,N</i> -dimethyl formamide	0.463	10 309 <sup>c</sup>	185
dimethyl sulfoxide	0.438	10 080	

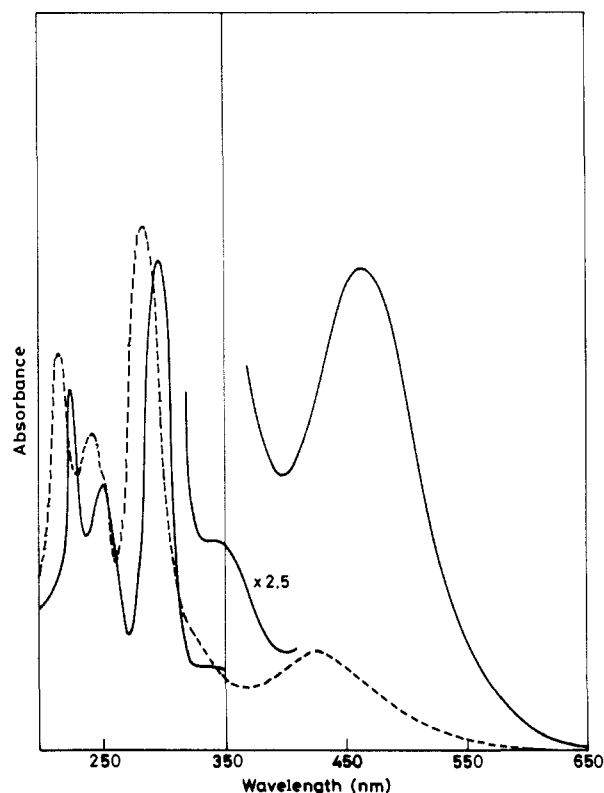
<sup>a</sup> Tetraphenylborate salt; the spectra obtained for the solid in acetonitrile was identical with that for species generated in situ by [Fe(bpy)<sub>3</sub>]<sup>3+</sup> oxidation in acetonitrile; Typical concentration  $\sim 5 \times 10^{-3}$  M. <sup>b</sup> Taken from Koppel, I. A.; Palm, V. A. In *Advances in Linear Free Energy Relationships*; Chapman, N. B., Shorter, J., Eds.; Plenum: London, 1972; pp 254–258. <sup>c</sup> The compound decomposes in DMF solution as seen from the extinction coefficient value viz., 185 M<sup>-1</sup> cm<sup>-1</sup>.

**Figure 1.** Electronic spectrum of [(bpy)<sub>2</sub>Ru(NCS)Cl] in (a) acetonitrile and (b) methylene chloride. The shoulder toward the higher energy side is clearly visible in methylene chloride.

at around 340 nm is, however, nonsolvatochromic.

The completely oxidized (33) dimers show a largely blue shifted band as expected<sup>23</sup> (Figure 2), and the extinction coefficient values of the different bands increase 2–3-fold.

The mixed-valence dimer [Cl(bpy)<sub>2</sub>RuNCSRu(bpy)<sub>2</sub>Cl]<sup>2+</sup> showed a weak, broad, and unsymmetrical intervalence transfer

**Figure 2.** Electronic spectra of (22) (—) and (33) (---) compounds of [Cl(bpy)<sub>2</sub>RuNCSRu(bpy)<sub>2</sub>Cl]<sup>n+</sup> in acetonitrile.**Table IV.** NIR Spectral Data for [Cl(bpy)<sub>2</sub>RuNCSRu(bpy)<sub>2</sub>X]<sup>2+</sup><sup>a</sup>

X <sup>-</sup>	$\bar{\nu}_{IT}$ (cm <sup>-1</sup> )	$\epsilon_{IT}$ (M <sup>-1</sup> cm <sup>-1</sup> )	$\Delta\bar{\nu}_{1/2}$ (calcd) <sup>c</sup> (cm <sup>-1</sup> )	$\Delta\bar{\nu}_{1/2}$ (obsd) (cm <sup>-1</sup> )
Cl <sup>-</sup>	10 638	411	4959	5464
NCS <sup>-b</sup>	13 605	36	5605	4565
NO <sub>2</sub> <sup>-b</sup>	12 195	150	5307	4845

<sup>a</sup> Spectra recorded in acetonitrile solutions; typical concentration  $\sim 10^{-3}$ – $10^{-4}$  M. <sup>b</sup> The mixed-valence species was generated in situ in acetonitrile solution by [Fe(bpy)<sub>3</sub>]<sup>3+</sup> oxidation. <sup>c</sup> The full width at half maximum was calculated by using the Hush model (see text).

band at around 950 nm which is absent in both the (22) and (33) compounds (Figure 4). The solvatochromism (Table III) exhibited by this band conformed well with the model proposed by Hush<sup>17</sup> for class II mixed-valence compounds. The plot of  $E_{op}$  versus  $[(1/n^2) - (1/D)]$ ,<sup>34</sup> where  $n^2$  and  $D$  are optical and static

(34) A deviation was observed in the case of water as the solvent. This effect has been attributed to the smallness of the water molecule, which can penetrate somewhat between the planar 2,2'-bipyridine ligands. In that case, the dielectric continuum approximation used to predict the linear relationship is not fully appropriate, see ref 32.

**Table V.** Characteristic Parameters Calculated from IT Bands and Hush Formulas for  $[\text{Cl}(\text{bpy})_2\text{RuNCSRu}(\text{bpy})_2\text{Cl}]^{2+}$ <sup>a,b</sup>

solvent	$\bar{\nu}_{\text{IT}}$ ( $\text{cm}^{-1}$ )	$\epsilon_{\text{IT}}$ ( $\text{M}^{-1} \text{cm}^{-1}$ )	$\Delta\bar{\nu}_{1/2}(\text{exp})$ ( $\text{cm}^{-1}$ )	$\Delta\bar{\nu}_{1/2}(\text{calcd})^c$ ( $\text{cm}^{-1}$ )	$f \times 10^2$ <sup>c</sup>	$D^c$ ( $\text{\AA}$ )	$ M  \times 10^{10}$ <sup>c</sup> ( $\text{\AA}$ esu)	$\lambda_i^c$ ( $\text{cm}^{-1}$ )	$\lambda_o^c$ ( $\text{cm}^{-1}$ )	$H_{\text{AB}}^c$ ( $\text{cm}^{-1}$ )	$\alpha^2 \times 10^3$ <sup>c</sup>
acetonitrile	10 638	411	5464	4959	1.03	0.299	1.436	7265	3487	453	1.85
acetone	10 417	387	6286	4905	1.12	0.315	1.513	7265	3258	466	2.02

<sup>a</sup>Tetraphenylborate salt. <sup>b</sup>For various parameters see the text. <sup>c</sup>Calculated by using "Hush formulas".

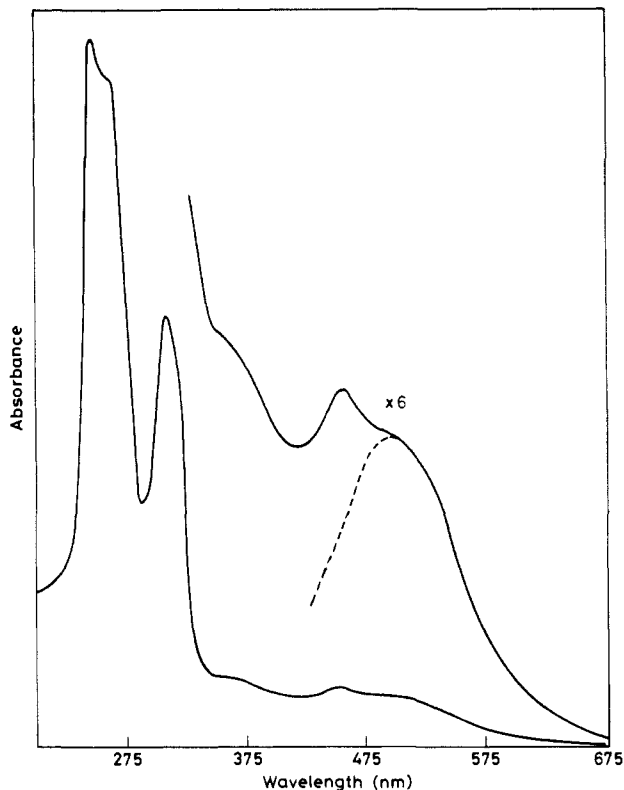


**Figure 3.** Electronic spectrum of  $[\text{Cl}(\text{bpy})_2\text{RuNCSRu}(\text{bpy})_2(\text{NCS})]\text{-BPh}_4$  in acetonitrile. The shoulder toward the lower energy side is prominent, and the dashed line shows the band profile assuming a gaussian shape.

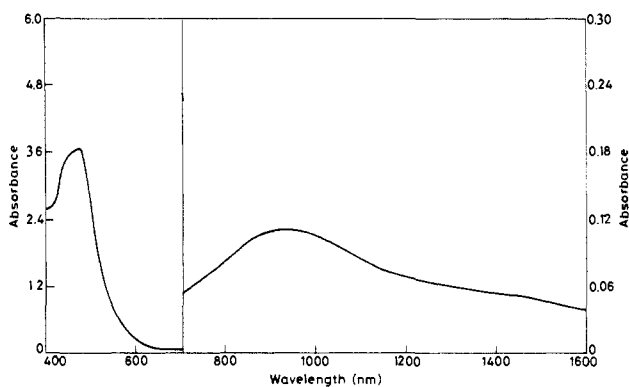


**Figure 4.** NIR and visible spectrum of  $[\text{Cl}(\text{bpy})_2\text{RuNCSRu}(\text{bpy})_2\text{Cl}]^{2+}$  in acetonitrile. The concentration used was  $10^{-3}$  M.

dielectric constants, is linear. The inner sphere ( $\lambda_i$ ) and outer sphere ( $\lambda_o$ ) reorganizational energies were calculated from the intercept and slope of this plot, respectively. The calculated bandwidth of the IT band according to the Hush model was slightly lower ( $\sim 10\%$  in acetonitrile and  $\sim 20\%$  in acetone) than the experimentally observed one<sup>19,35,36</sup> (Table IV). The interaction parameter,  $H_{\text{AB}}$ , and delocalization factor,  $\alpha^2$ , calculated from

(35) Sutton, J. E.; Sutton, P. M.; Taube, H. *Inorg. Chem.* **1979**, *18*, 1017.

(36) This suggests that the interaction between the metal centers is weak which is corroborated by the magnitudes of the delocalization and interaction parameters, viz.,  $\alpha^2$  and  $H_{\text{AB}}$ .

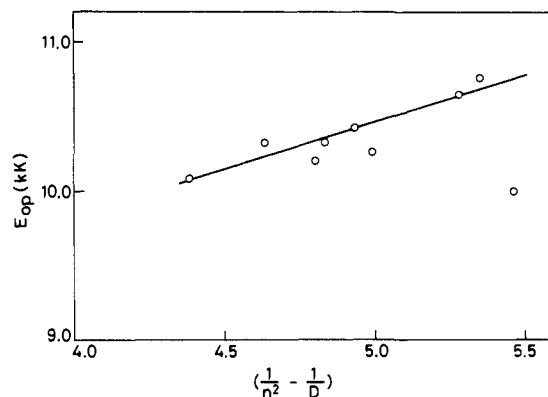


**Figure 5.** Plot of  $(\frac{1}{n^2} - \frac{1}{D})$  versus  $E_{\text{op}}$  for the IT transition of  $[\text{Cl}(\text{bpy})_2\text{RuNCSRu}(\text{bpy})_2\text{Cl}]^{2+}$  ion (see ref 34).

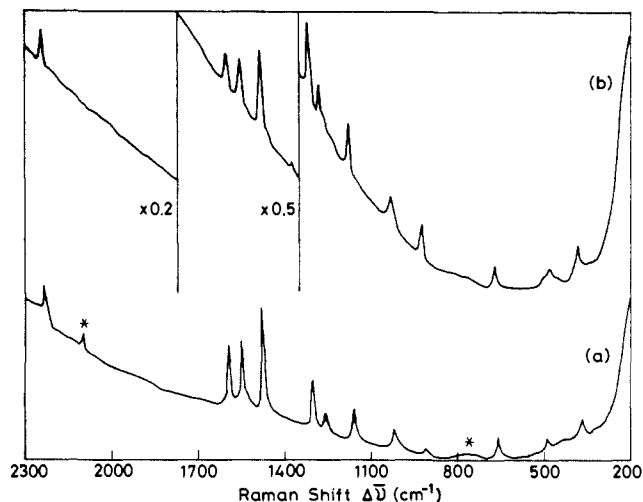


**Figure 6.** Resonance Raman spectra of  $[\text{Cl}(\text{bpy})_2\text{RuNCSRu}(\text{bpy})_2\text{Cl}]\text{-BPh}_4$  in acetonitrile with (a) 457.9 and (b) 514.5 nm excitation wavelengths. Intensity reference is the  $2249 \text{ cm}^{-1}$  ( $\nu(\text{CN})$ ) band of the acetonitrile solvent. Spectral slitwidth (a) 6 and (b)  $8 \text{ cm}^{-1}$ . Laser power: 100 mW. The peaks marked with asterisks are the vibrational modes due to thiocyanate ion.

intervalence transfer band parameters are respectively  $453 \text{ cm}^{-1}$  and  $1.85 \times 10^{-3}$  in acetonitrile and are comparable with those of the other reported compounds.<sup>16</sup> The quantities like oscillator strength, dipole strength, and transition dipole moment were calculated by using the equations given elsewhere<sup>16,19</sup> and are given in Table V. A metal-to-metal separation of  $7 \text{ \AA}$  was used for the calculations.<sup>37</sup>

Emission spectra for  $[(\text{bpy})_2\text{Ru}(\text{NCS})\text{Cl}]$  and  $[\text{Cl}(\text{bpy})_2\text{RuNCSRu}(\text{bpy})_2\text{Cl}]$  were obtained and are illustrated in Figure 8. The excitation sources were the  $\text{Ar}^+$  laser lines. The spectra were uncorrected for instrumental factors. Due to the local burning of the samples by the laser, the evaluation of emission quantum yields presented difficulties. However, an upper limit of  $\Phi_{\text{em}} \ll 0.01$  was obtained, and hence the compounds seem to be weak emitters. However, from the relative intensities of the emission bands, the dimer emission is approximately 5–10-fold<sup>38</sup>

(37) Various interatomic distances of the  $[\text{RuNCSRu}]$  unit taken from the X-ray data are reported in ref 33, from which approximate values for the metal-to-metal separation was deduced.

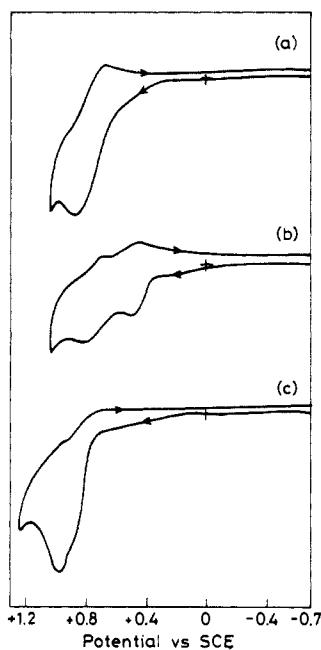


**Figure 7.** Cyclic voltammograms for the oxidations of monomeric and dimeric compounds in methylene chloride. Supporting electrolyte, TBAP: (a)  $[(bpy)_2Ru(NCS)Cl] \cdot 2H_2O$ , (b)  $[(bpy)_2Ru(NCS)_2]$  (scan rate =  $200 \text{ mV s}^{-1}$ ), and (c)  $[Cl(bpy)_2RuNCSRu(bpy)_2Cl]BPh_4$  (scan rate:  $100 \text{ mV s}^{-1}$ ). The shoulders in the case of (c) are clearly visible in higher scan rates.

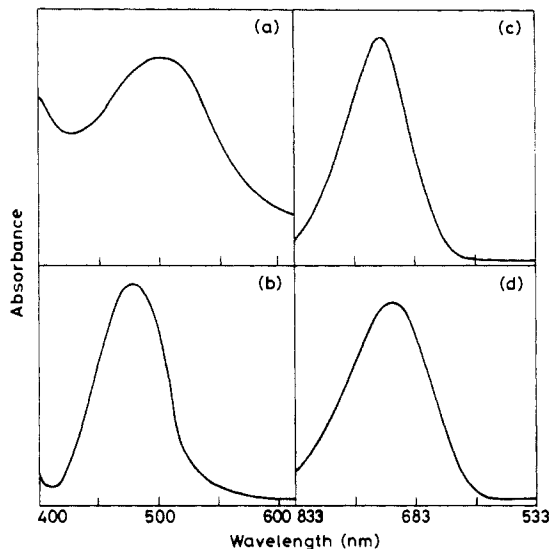


**Figure 8.** Absorption (a) and emission (c) spectra of  $[(bpy)_2Ru(NCS)Cl]$  and absorption (b) and emission (d) spectra of  $[Cl(bpy)_2RuNCSRu(bpy)_2Cl]BPh_4$  in acetonitrile. The  $\lambda_{ex}$  for emission spectra is  $457.9 \text{ nm}$ .

less than that of the monomer. This could be due to the coordination of the second  $[(bpy)_2Ru]^{2+}$  unit in the dimeric complex. The withdrawal of electron density by the second  $[Ru(bpy)_2]^{2+}$  unit from the first metal center and thereby providing pathway for a nonradiative deactivation of the emissive state could be a reason for the weaker emission observed for the dimer.<sup>39,40</sup> Such an effect of the coordination of the second  $[Ru(bpy)_2]^{2+}$  unit has been reported recently by several investigators.<sup>39,41-43</sup> Further,

(38) The emission spectra were recorded under identical conditions after approximately equal time intervals from the mounting of the samples. The band intensities were calculated from the uncorrected spectra. This is taken to be proportional to the emission efficiency assuming a constant local burning (see ref 20).

(39) (a) Fuchs, Y.; Lofters, S.; Dieter, T.; Shi, W.; Morgan, R.; Streckas, T. C.; Gafney, H. D.; Baker, A. D. *J. Am. Chem. Soc.* **1987**, *109*, 2691. (b) Braunstein, C. H.; Baker, A. D.; Streckas, T. C.; Gafney, H. D. *Inorg. Chem.* **1984**, *23*, 857.

**Table VI.** Resonance Raman Spectral Data<sup>a</sup>

$[Ru(bpy)_2(NCS)Cl] \cdot 2H_2O$		$[Cl(bpy)_2RuNCSRu(bpy)_2Cl]BPh_4$	
$\lambda_{ex} = 514.5 \text{ nm}$	$\lambda_{ex} = 457.9 \text{ nm}$	$\lambda_{ex} = 514.5 \text{ nm}$	$\lambda_{ex} = 457.9 \text{ nm}$
379 (0.8)	378 (0.6)	373 (3.4)	375 (3.5)
489 (0.8) <sup>b</sup>	485 (1.3) <sup>b</sup>	487 (0.6) <sup>b</sup>	486 (0.6) <sup>b</sup>
661 (0.7)	661 (0.7)	660 (0.6)	663 (0.7)
	808 <sup>c</sup> (1.0)	777 <sup>c</sup> (br)	
1021 (0.7)	1020 (0.4)	1035 (1.8)	1035 (2.3)
1035 (0.6)			
1163 (1.7)	1160 (0.8)	1157 (2.3)	1159 (3.3)
1265 (0.8)	1265 (0.4)	1279 (2.0)	1280 (3.0)
1307 (2.1)	1310 (1.1)	1321 (3.3)	1320 (5.4)
1486 (6.1)	1485 (3.9)	1482 (6.8)	1480 (9.2)
1560 (3.5)	1558 (2.4)	1554 (2.9)	1555 (3.9)
1606 (2.2)	1603 (1.1)	1598 (3.1)	1600 (4.9)
	2120 <sup>c</sup> (1.2)	2146 <sup>c</sup> (w)	

<sup>a</sup>Spectra recorded by using capillaries in acetonitrile solutions. The relative intensity values in parentheses were calculated with reference to the  $\nu(CN)$  band of acetonitrile. <sup>b</sup>The peak at around  $485 \text{ cm}^{-1}$  is very broad. <sup>c</sup>Peaks are due to coordinated thiocyanate ions.

the excitation spectra of these emission for monomer and dimer suggests that within the interval of  $457.9\text{--}514.5 \text{ nm}$ , the excitation leads to the population of the same emissive state. This fluorescent state seems to be localized on the 2,2'-bipyridine coligands as borne out by the resonance Raman studies (vide supra). This is further substantiated by two more observations: (i) the shift in the emission maxima was relatively small when going from the monomer to dimer, and (ii) the solvatochromism associated with this emission maximum suggests that the emissive state is mostly localized on the 2,2'-bipyridine coligands.

**Resonance Raman Spectra.** Earlier studies<sup>39,41-43</sup> show that the laser excitations in the intense visible absorption bands of bis- and tris(polypyridyl)ruthenium(II) complexes yield detailed resonance Raman spectra above  $1000 \text{ cm}^{-1}$ , characteristic of the coordinated polypyridyl vibrations. Excitation of  $[Ru(bpy)_3]^{2+}$ <sup>44</sup> using different  $Ar^+$  laser lines that overlap the MLCT absorption to different degrees yielded an excitation independent seven line characteristic pattern for the coordinated 2,2'-bipyridine ligand. In contrast, detailed studies on the resonance Raman spectra of bis(bipyridyl)ruthenium(II) complexes having various diimine bridging ligands showed marked dependence<sup>39</sup> on the excitation wavelengths. Depending on the excitation within the two different visible absorption bands corresponding to the two different MLCT's terminating at the  $\pi^*$  orbitals of the 2,2'-bipyridine coligand and the bridging diimines, the corresponding vibrational modes were found to be enhanced in intensity. Thus, an unambiguous assignment of the visible absorption bands was possible.

Such an exercise was not possible in our case, as the MLCT transitions associated with the 2,2'-bipyridine and the bridging thiocyanate ligand were overlapping to a large extent. However, excitation of the monomeric and dimeric compounds, at least, in two different wavelengths within the  $Ar^+$  laser lines yielded convincing results. Excitation of  $[(bpy)_2Ru(NCS)Cl]$  at  $514.5$

(40) The tris(bipyridine) complex of Ru(II) is luminescent, and when the strongly electron-withdrawing  $NO_2$  is substituted at the 4-position of bpy, the  $\pi^*$  orbital is lowered in energy by  $3750 \text{ cm}^{-1}$ . From the RR spectral studies,<sup>41a</sup> the excited state of the MLCT was found to have a significant portion of the charge localized on the nitro groups. Since  $NO_2$  groups are strongly coupled to the solvent molecules, the fluorescence of the tris(nitrobipyridine) complex of Ru(II) is quenched by an efficient radiationless deactivation. In a dinuclear complex, the second metal center can act similarly, and depending on the extent of coupling between the metal centers the emissive state can be partially or fully quenched.<sup>39a</sup>

(41) (a) Basu, A.; Gafney, H. D.; Streckas, T. C. *Inorg. Chem.* **1982**, *21*, 1085. (b) Haga, M. A. *Inorg. Chim. Acta* **1980**, *45*, L183.

(42) (a) Rillema, D. P.; Mack, K. B. *Inorg. Chem.* **1982**, *21*, 3849. (b) Rillema, D. P.; Callahan, R. W.; Mack, K. B. *Inorg. Chem.* **1982**, *21*, 2589.

(43) (a) Dallinger, R. F.; Woodruff, W. H. *J. Am. Chem. Soc.* **1979**, *101*, 4391. (b) Bradley, P. G.; Kress, N.; Hornberger, B. A.; Dallinger, R. F.; Woodruff, W. H. *J. Am. Chem. Soc.* **1981**, *103*, 7441. (c) Basu, A.; Gafney, H. D.; Streckas, T. C. *Inorg. Chem.* **1982**, *21*, 2231.

(44) Smothers, W. K.; Wrighton, M. S. *J. Am. Chem. Soc.* **1983**, *105*, 1067.

**Table VII.** Electrochemical Data for the Bis(bipyridyl)ruthenium(II) Complexes in Methylene Chloride

complex	oxidations <sup>a,b</sup>		reductions <sup>a,c</sup>	
	$E_{1/2}$ (1)	$E_{1/2}$ (2)	$E_{1/2}$ (3)	$E_{1/2}$ (4)
[Ru(bpy) <sub>2</sub> (NCS)Cl]	+0.80 (84)	+1.07 (84)	-1.41 (83)	-1.69 (63)
[Ru(bpy) <sub>2</sub> (NCS) <sub>2</sub> ]	+0.51 (61)	+0.77 (76)	-1.41 <sup>d</sup>	-1.60 <sup>d</sup>
[Cl(bpy) <sub>2</sub> RuNCSRu-(bpy) <sub>2</sub> Cl]BPh <sub>4</sub>	+0.82 <sup>d</sup>	+0.97 <sup>d</sup>	-1.42 <sup>d</sup>	-1.66 <sup>d</sup>

<sup>a</sup>The potential values in volts are referred to SCE at room temperature. The error is  $\pm 0.02$  V. <sup>b</sup> $\Delta E_p$  values are given in parentheses and were extrapolated from the intercepts of the plots of  $\Delta E_p$  versus  $\nu^{1/2}$ , where  $\nu$  is scan rate. <sup>c</sup>The reduction waves are due to the 2,2'-bipyridine ligands. <sup>d</sup>Overlapping waves.

nm ( $\nu_o - \nu_e = 485 \text{ cm}^{-1}$ )<sup>45</sup> yielded an RR spectrum having bands characteristic of the 2,2'-bipyridine vibrational modes, along with a few low-energy bands (cf. Table VI) attributable to the  $\nu(\text{Ru-N})$  modes of the 2,2'-bipyridine unit. When the compound was excited with a 457.9 nm ( $\nu_o - \nu_e = 1920 \text{ cm}^{-1}$ ) laser line, the RR spectrum contained bands at 2120  $\text{cm}^{-1}$ , 810  $\text{cm}^{-1}$  (broad and weak) along with the characteristic 2,2'-bipyridine vibrations, which were somewhat reduced in intensity (cf. Table VI). The excitations, with 457.9 nm ( $\nu_o - \nu_e = 147 \text{ cm}^{-1}$ ) and 514.5 nm ( $\nu_o - \nu_e = 2545 \text{ cm}^{-1}$ ) laser lines, of the dimeric compound yielded the 2,2'-bipyridine vibrations with considerably varying intensities. However, the excitation of the dimer at 514.5 nm yielded the band due to the  $\nu(\text{CN})$  mode at around 2146  $\text{cm}^{-1}$  and a broad weak band at around 777  $\text{cm}^{-1}$  attributable to the  $\nu(\text{CS})$  mode of the bridging NCS group. Lack of excitation facilities at further higher or lower energies of the overlapping MLCT transitions did not allow us to probe this point more clearly.

**Electrochemistry.** The essential electrochemical redox potentials are given in Table VII. The peak potentials are scan rate dependent. Plots of  $\Delta E_p$ , where  $\Delta E_p = E_{p,a} - E_{p,c}$  versus  $\nu^{1/2}$ , where  $\nu$  is the scan rate, were found to be linear with intercept values ranging from 60 to 85 mV (Figure 7).<sup>46,47</sup> Although, there seems to be certain quasireversibility in some of the processes ( $i_{pa}/i_{pc} \neq 1$ ), all the redox processes conform to a one-electron change. The monomeric compounds, apart from the Ru(II)/Ru(III) couples, yield a second oxidation wave and the corresponding cathodic part (cf. Figure 7, Table VII). Since the ligands could not be oxidized at these potentials, this second oxidation is assigned tentatively to the oxidation of Ru(III) to Ru(IV). Efforts to separate the Ru(IV) species by chemical oxidation are underway.

The thiocyanate bridged dimeric compound shows two overlapping waves, with a single maximum resolved for both the oxidation and the reduction processes, the other appearing as clear shoulder. The first oxidation process of (22) dimer is reversible, while the successive oxidation of (23) to (33) seems to be quasireversible. The lesser interaction (see Discussion) between the two metal centers and hence the instability of the mixed-valence species could give rise to other side reactions, thereby affecting the reversibility of this redox process. The comproportionation quotient ( $K_{\text{com}}$ ) for the reaction 1 was calculated by using the separation between the two redox stages and is 350.

## Discussion

The integrated intensity values for the  $\nu(\text{CN})$  band have been calculated on earlier occasions. A value of  $10.1 \times 10^4 \text{ M}^{-1} \text{ cm}^{-2}$ <sup>30</sup> has been reported for [(bpy)<sub>2</sub>Ru(NCS)<sub>2</sub>]. The calculated value for [(bpy)<sub>2</sub>Ru(NCS)Cl] is  $12 \times 10^4 \text{ M}^{-1} \text{ cm}^{-2}$  which is conclusive proof<sup>33</sup> for the presence of the N-bonded linkage isomer. Though the occurrence of N-bonded thiocyanate in mixed ligand complexes with  $\pi$ -acceptor (soft) bases with "class b" (soft) metal ions, like

Ru(II), is perfectly logical, the formation of the other linkage isomer cannot be strictly ruled out. On several earlier occasions, it has been observed that the reaction of  $[\text{M}(\text{NH}_3)_5\text{H}_2\text{O}]^{2+}/[\text{M}(\text{NH}_3)_5\text{X}]^{2+}$ ,<sup>28,29a,48,49</sup> where M = Ru, Co; X = Cl, Br, I, with chalcogenocyanate ions yielded both the linkage isomers, even though the coligands ( $\sigma$ -donor) could favor only the S- or Se-bonded isomers. Hence, it is presumed that the formation of the N-bonded linkage isomer dominates the process by virtue of the excellent  $\pi$ -acceptor qualities of the 2,2'-bipyridine coligand.

Although a change in the bonding properties of the  $\pi$ -acceptor ligands in going from [(bpy)<sub>2</sub>Ru(NCS)<sub>2</sub>] to [(bpy)<sub>2</sub>Ru(NCS)Cl] is obvious, as reflected from the oxidation potentials of the Ru(II)/Ru(III) couple of these compounds, viz., +0.51 and +0.80 V respectively, only a small blue shift of about 600  $\text{cm}^{-1}$  in the position of the band due to  $d\pi(\text{Ru})-\pi_1^*(\text{bpy})$  MLCT is observed. This suggests that considerable stabilization of the metal  $\pi$ -orbitals and a slight destabilization of the  $\pi^*$  orbital of the 2,2'-bipyridine ligand is accompanied by the introduction of a  $\sigma$ -donor ligand like chloride ion. A similar trend was noted for the selenocyanate analogues of these compounds.<sup>20</sup> As for the  $\pi$ -acceptor properties, there is not much difference between the two chalcogenocyanate ions. However, the available evidence suggests that the selenocyanate ion has a slightly favorable edge over the thiocyanate ion. This is further corroborated by the fact that the  $\pi$ -acceptor orbitals of the chalcogenocyanate ions ( $3\pi^*$  degenerate orbitals)<sup>50</sup> are localized on the central carbon atom and the contributions of both the end atoms, viz., N and S or Se are very little.<sup>19,51</sup>

A red shift of approximately 3000  $\text{cm}^{-1}$  is associated with the  $d\pi(\text{Ru})-3\pi^*(\text{NCS}^-)$  MLCT transition, when going from the monomeric [(bpy)<sub>2</sub>Ru(NCS)Cl] to the dimeric [Cl-(bpy)<sub>2</sub>RuNCSRu(bpy)<sub>2</sub>Cl]BPh<sub>4</sub>. This is attributed to the stabilization of the  $3\pi^*$  acceptor orbitals of the thiocyanate ligand due to the coordination of the second [(bpy)<sub>2</sub>Ru]<sup>II</sup> unit on the free sulfur end of the thiocyanate ligand. In spite of this, a large stabilization of around 7000–8000  $\text{cm}^{-1}$ , due to greater interaction between the metal centers through the bridging ligands, has been observed for some diimine bridging ligands.<sup>39</sup> This suggests that in the case of the thiocyanate bridge the interaction between the metal centers is only moderate. The extent of  $\pi$ -back donation into the acceptor  $3\pi^*$  antibonding orbitals of the thiocyanate bridge, which is a key factor in determining the extent of metal-to-metal interaction in these compounds, is very low due to the presence of the strongly competing  $\pi$ -acceptor 2,2'-bipyridine coligands.<sup>19,20</sup> Besides, the first antibonding orbital of the 2,2'-bipyridine and the degenerate  $3\pi^*$  antibonding acceptor orbitals of the thiocyanate ligand seem to be very close in energies. The resonance Raman studies gave a valuable clue for this. The residual intensities of the coordinated 2,2'-bipyridine vibrations in the resonance Raman spectra obtained with excitation within the ruthenium to thiocyanate MLCT transition is greater than that could be predicted on the basis of the excitation wavelength separation from the MLCT absorption of the 2,2'-bipyridine coligands. In fact, the excited state of the lowest energy MLCT transition is delocalized over both the ligands, 2,2'-bipyridine and the bridging ligand; thiocyanate ion and this could arise due to their closeness in energy. The metal-to-thiocyanate charge-transfer depletes the charge on the metal center, and as a result all the other M-ligand units will receive lower charge and vice-versa. This can cause a RR effect for all of the symmetrical vibrational modes of the other ligands, even when the excitation was done within a particular CT band.<sup>52</sup> The closeness of the acceptor orbital energies of 2,2'-bipyridine and thiocyanate could augment this phenomenon thereby yielding the observed RR spectra.

(45) ( $\nu_o - \nu_e$ ) denotes the separation between the exciting laser line and the absorption maximum of the lowest energy CT band in visible electronic spectrum.

(46) Nicholson, R. S.; Shain, I. *Anal. Chem.* **1964**, *36*, 706.

(47) The separation between the cathodic and anodic peaks are generally higher than the theoretical value 59 mV. However, the linearity of the  $\Delta E_p$  versus  $\nu^{1/2}$  plots, the intercept values of these plots (60–85 mV), and the closeness of  $i_{pa}/i_{pc}$  to unity are taken as the criterion for one-electron reversible processes.

(48) Jackson, W. G.; Hookey, C. N. *Inorg. Chem.* **1984**, *23*, 668.

(49) Jackson, W. G.; Jurisson, S. S.; McGregor, B. C. *Inorg. Chem.* **1985**, *24*, 1788.

(50) Rabalais, J. W.; McDonald, J. M.; Sherr, V.; McGlynn, S. P. M. *Chem. Rev.* **1971**, *71*, 73.

(51) di Sipio, L.; Oleari, L.; de Michelis, G. *Coord. Chem. Rev.* **1966**, *1*, 7.

(52) Balk, R. W.; Snoeck, T.; Stufkens, D. J.; Oskam, A. *Inorg. Chem.* **1980**, *19*, 3015.

The mixed-valence species  $[\text{Cl}(\text{bpy})_2\text{RuNCSRu}(\text{bpy})_2\text{Cl}]^{2+}$  exhibits much less stability compared to that of the  $[\text{Ru}(\text{NH}_3)_5]^{n+}$  and  $[\text{Fe}(\text{CN})_5]^{n-}$  analogues, as seen from their comproportionation constant values.<sup>53</sup> The overall stability of the mixed-valence species could be attributed to several factors:<sup>14,16,35,54-56</sup> (i) stabilization due to the delocalization of the optical electron; (ii) stabilization due to purely electrostatic factors; (iii) stabilization due to variation in structural parameters when going from isovalent to mixed-valence species; (iv) stabilization due to variation in the magnetic interaction between the two paramagnetic centers via a "superexchange"<sup>57</sup> pathway; and (v) stabilization due to inductive effect of 3+ charge discussed in ref 35. However, the factors contributing to a large extent are  $\Delta G^\circ_{\text{del}}$  and  $\Delta G^\circ_{\text{coul}}$ .<sup>19,35,55</sup>

It has been suggested recently that the contribution of the  $\Delta G^\circ_{\text{coul}}$  term could be relatively larger in the case of the anionic ligand-bridged mixed-valence compounds than that in the case of neutral ligand-bridged compounds.<sup>14,19</sup> For strongly interacting systems, the contribution of the  $\Delta G^\circ_{\text{del}}$  term is large.<sup>16,19</sup> However, in the thiocyanate- and selenocyanate-bridged compounds the contribution due to the  $\Delta G^\circ_{\text{del}}$  term seems to be controversial. As discussed earlier, the strongly competitive  $\pi$ -acceptor properties of the 2,2'-bipyridine could affect the extent of delocalization via the thiocyanate bridge. This is reflected in the calculated delocalization factor ( $\alpha^2$ ) values as given below

complex	$\alpha^2$
$[(\text{NH}_3)_5\text{Ru-NCS-Ru}(\text{NH}_3)_5]^{4+}$	delocalized <sup>18</sup>
$[(\text{CN})_5\text{Fe-NCS-Fe}(\text{CN})_5]^{6-}$	$5.3 \times 10^{-3}$ <sup>19</sup>
$[(\text{CN})_5\text{Fe-NCS-Fe}(\text{CN})_5]^{6-}$	$5.0 \times 10^{-3}$ <sup>19</sup>
$[\text{Cl}(\text{bpy})_2\text{Ru-NCS-Ru}(\text{bpy})_2\text{Cl}]^{2+}$	$1.85 \times 10^{-3}$
$[\text{Cl}(\text{bpy})_2\text{Ru-NCS-Fe}(\text{bpy})_2\text{Cl}]^{2+}$	$1.90 \times 10^{-3}$ <sup>20</sup>
$[\text{Cl}(\text{bpy})_2\text{Ru-Pyz-Ru}(\text{bpy})_2\text{Cl}]^{3+}$	$2.6 \times 10^{-3}$ <sup>22</sup>

In asymmetric class II systems, a thermodynamic barrier  $\Delta E$  to both optical and thermal electron transfer is introduced in addition to the outer and inner sphere reorganizational energies, thus

$$E_{\text{op}} = \lambda + \Delta E$$

$$\lambda = \lambda_i + \lambda_o$$

This barrier can be qualitatively estimated from the deviation of the IT spectral bandwidth from that of the calculated one from the Hush model. The position and the acceptable closeness of the observed and calculated (using Hush model) bandwidths of the IT band is suggestive of the pseudosymmetry<sup>19</sup> present in the otherwise asymmetric thiocyanate bridge. Given that the  $3\pi^*$  acceptor orbitals of the thiocyanate bridge is localized on the central carbon atom,<sup>19,51</sup> the  $\pi$ -system through which the electron is mediated is, qualitatively, similar to any other symmetric class II mixed-valence compounds.

(53) The comproportionation constant values for  $[(\text{CN})_5\text{FeNCXFe}(\text{CN})_5]^{6-}$ , where X = S or Se, are 1474 and 2399, respectively. For  $[(\text{NH}_3)_5\text{RuNCSRu}(\text{NH}_3)_5]^{4+}$ ,  $K_{\text{com}}$  is 4075.<sup>19</sup>

(54) Gagne, R. R.; Spiro, C. L.; Smith, T. J.; Hamann, C. A.; Thies, W. R.; Shiemke, A. K. *J. Am. Chem. Soc.* **1981**, *103*, 4073.

(55) Sutton, J. E.; Taube, H. *Inorg. Chem.* **1981**, *20*, 3125.

(56) Pherlps, J.; Bard, A. J. *Electrochim. Acta* **1976**, *68*, 313.

(57) The "super-exchange pathway" has been observed to be efficient in the case of monoatomic bridges such as  $\text{O}^{2-}$ . This could be neglected in the case of triatomic bridges as in our case.

The electrochemical results indicate that the binuclear complex undergoes two successive one-electron oxidations, with the two oxidations occurring within a very short potential range. One would then expect the longer chain polymers to exhibit multielectron redox properties within a relatively shorter span of potentials. This may be a desirable property for utilization of these compounds as catalysts for multielectron transfer processes. As the thiocyanate ion has capabilities to be a bridging ligand in several linear chain and three-dimensional polymeric transition-metal complexes,<sup>58</sup> the synthesis of appropriate thiocyanate-bridged compounds, those can be used as multielectron transfer catalysts, could be planned in future.

**Conclusion.** The coordination of a second  $[(\text{bpy})_2\text{Ru}]^{n+}$  on the free sulfur end of the  $[(\text{bpy})_2\text{RuCl}(\text{NCS})]$  reduces the fluorescence by 5–10-fold suggesting the presence of a moderate metal-to-metal interaction via the thiocyanate bridge. The observed position of the IT band for the corresponding mixed-valence species, which is comparable with that of the other symmetric class II mixed-valence compounds, such as  $[\text{Cl}(\text{bpy})_2\text{Ru}(\mu\text{-L})\text{Ru}(\text{bpy})_2\text{Cl}]^{3+}$  where L = pyz, 4,4'-bpy, suggests that the thermodynamic barrier for the electron transfer due to the intrinsic asymmetry of the thiocyanate ion is not large. This is explained in terms of the delocalization of the optical electron via pseudosymmetric  $\pi$ -overlap, that is,  $d\pi(\text{M})-3\pi^*(\text{NCS})-d\pi(\text{M})$ .<sup>59</sup> Further, this interaction across the thiocyanate ion could be "tuned" as to our needs by judiciously varying the coligands on the metal centers (in terms of  $\sigma/\pi$ -acceptor/-donor properties). This might have a good impact on the development of redox catalysts for several important multielectron processes as water oxidation.

**Acknowledgment.** We thank Prof. V. Krishnan, Indian Institute of Science, Bangalore, India, who helped in getting the NIR spectra. One of the authors (V.P.) acknowledges Council of Scientific and Industrial Research (CSIR), New Delhi, India, for a Senior Research Fellowship. Thanks are also due to Dr. O. K. Medhi, Chemistry Department, Gauhati University, India, for his help in making some electrochemical measurements.

(58) (a) Manoli, J. M.; Potvin, C.; Secheresse, F.; Marzak, S. *J. Chem. Soc., Chem. Commun.* **1986**, 1557. (b) Taniguchi, M.; Sugita, Y.; Ouchi, A. *Bull. Chem. Soc. Jpn.* **1987**, *60*, 1321. (c) Nakao, Y.; Nakamura, H.; Mori, W.; Sakurai, T.; Suzuki, S.; Nakahara, A. *Bull. Chem. Soc. Jpn.* **1986**, *59*, 2755.

(59) Apart from this LUMO ( $3\pi^*$ ) of the thiocyanate ion, Taube<sup>60</sup> has suggested the possibility of the interaction of the HOMO ( $2\pi$ )<sup>50</sup> with the  $d\pi$  orbitals of the metal centers having appropriate symmetry. The participation of the LUMO could be thought of as giving rise to a high-energy virtual MLCT state<sup>61</sup> such as  $\text{M}^+-\text{L}^--\text{M}(E_1)$ . The HOMO interaction could be thought of as giving rise to similar LMCT,<sup>61</sup>  $\text{M-L}^+-\text{M}^2(E_2)$ . The delocalization of the optical electron can be explained by the mixing of these "localized" high-energy states  $E_1$  and  $E_2$  with the ground state,  $\text{M-L}-\text{M}(E_0)$ . The  $E_1$  "assisted" delocalization should decrease as one goes from  $[\text{Ru}(\text{NH}_3)_5]^{n+}$ ,  $[\text{Fe}(\text{CN})_5]^{n-}$ , to  $[\text{Ru}(\text{bpy})_2]^{n+}$  as the  $\pi$ -acceptor ligands, such as  $\text{CN}^-$  and bpy, could effectively compete with  $\text{NCX}^-$  ion for  $\pi$ -bond compared to ammonia and thus decreasing the degree of delocalization. The reverse is the case if the delocalization is "assisted" by  $E_2$ . The observed decreasing trend in the  $\alpha^2$  values (see Discussion) suggests that the mechanism or at least the effective mechanism operative in these chalcogenocyanate bridged complexes must be the "localized" MLCT "assisted" delocalization.

(60) Taube, H., personal communication.

(61) (a) Mayoh, B.; Day, P. *Inorg. Chem.* **1974**, *13*, 2273. (b) Richardson, D. E.; Taube, H. *J. Am. Chem. Soc.* **1983**, *105*, 40.